

D/H RATIOS OF EARLY CRYSTALLISED AND LATE STAGE HYDROUS MINERALS IN MARTIAN METEORITE MIL 090136: TRACING THE SOURCE OF NAKHLITE Cl-RICH FLUID. L. J. Hallis¹, J. J. Barnes^{2,3,4} and I. A. Franchi². ¹School of Geographical and Earth Sciences, Gregory Building, University of Glasgow, Glasgow G12 8QQ. Email: lydia.hallis@glasgow.ac.uk, ²School of Physical Sciences, The Open University, Walton Hall, Milton Keynes MK7 6AA, ³NASA Johnson Space Center, 2101 E NASA Pkwy, Houston, TX 77058, U.S.A. ⁴Lunar and Planetary Laboratory, University of Arizona, 1629 E University Blvd, Tucson, AZ 85721, U.S.A.

Introduction: The nakhlites are currently the second most abundant group of martian meteorites available on Earth for study. Amphibole-bearing melt inclusions up to 350 μm diameter are present within the augite and olivine phenocrysts of two separate nakhlites - NWA 5790 and the Miller Range nakhlites [1-3]. Melt inclusion composition, along with the Cl, F and OH abundances of apatite, have been interpreted to suggest that both the nakhlites and chassignites formed during a single igneous event, where a Cl-rich exogenous fluid was added to the magma body during crystallization [2,4]. Apatite Cl, F and OH ratios suggest the fluid was added after crystallization of the chassignite olivine-hosted MIs, but prior to crystallization of chassignite intercumulus melt and of the nakhlites [2].

Although the timing of Cl-rich fluid addition to the chassignite/nakhlite pile has been investigated (e.g., [2,5]), the source of this fluid is still uncertain. The hydrogen isotope (D/H) ratios of the primary hydrous minerals apatite and amphibole within the amphibole-bearing nakhlites could indicate whether the exogenous Cl-rich fluid was magmatic in origin, or sourced from the martian surface/atmosphere. The aim of this study was to determine the D/H ratios of both amphibole and apatite within the nakhlite MIL 090136, in order to establish the source of the exogenous purported Cl-rich fluid added to the chassignite/nakhlite igneous sequence. In addition, comparisons of D/H ratios within apatite in early crystallized MIs vs. apatite within the mesostasis could indicate whether this nakhlite experienced degassing.

Methods: The Cameca Nanoscale Secondary Ion Mass Spectrometer (NanoSIMS) 50L at The Open University was used to measure the H abundances (expressed as equivalent amounts of H_2O) and H isotopic composition of target minerals following the protocols described in [6]. Three indium mounted standard apatite grains Ap003, Ap004, and Ap018 (as described by [7]), and a kaersutite composition amphibole standard (also in indium), containing 1.06 ± 0.07 wt.% (Francis McCubbin, NASA JSC, pers. Comm), were used for calibrating H_2O equivalent abundances in the unknowns [8]. A San Carlos olivine crystal, present in the indium mount along with apatite standards, was used to monitor the background contribution of H to the analyses, which equated to ~ 19 ppm H_2O for this

analytical session - corresponding to $<2\%$ of water content of the driest apatite analyzed. Ap004 with a δD value of -45 ± 5 ‰ [7] and the kaersutitic amphibole with a δD value -57 ± 13 ‰ (Francis McCubbin, NASA JSC, pers. comm.) were used for correcting the measured D/H ratios of unknowns for instrumental mass fractionation.

Results: *Mineralogy of MIL 090136 melt inclusions (MI).* The general mineralogy of the melt inclusions analysed here was previously described by [3]. Several olivine-hosted polycrystalline MI are present within thin-section MIL 090136,21, the largest of which (MI 1) is 110 μm diameter. In addition to Cl-rich amphibole, MI minerals include Al-Ti-rich augite, fayalitic olivine, alkali feldspar, glass, apatite and jarosite, as well as an Fe-Al-Ti-rich oxide (too small for definitive identification). Orthopyroxene was observed at one melt inclusion/olivine boundary. Amphibole is present in MI 1 and 2, with a potassic chlorohastingsite composition similar to that reported by [1-2] (Fig. 1). Several small anhedral apatite grains are also present in MI 2 - the largest being 4×4 μm , and the smallest being < 1 μm . The small size of these apatite grains prevented accurate compositional data collection. However, given the abundance of Cl within other MI phases, it is probable that MI 2 apatite is Cl-rich. In support of this, NanoSIMS ^{19}F isotope imaging (used to locate apatite for D/H ratio analyses) highlighted the lack of F enrichment in MI 2 apatite.

Composition of mesostasis apatite. Slightly larger apatite grains are present in the mesostasis of MIL 090136,21 and 090136,25 (up to 10×8 μm). Approximately half of these grains are euhedral, with an equant to tabular shape, whereas the others are anhedral. Mesostasis apatite is associated with both felsic glass and cristobalite, and is commonly intergrown with Ti-rich magnetite. The larger size of the mesostasis apatite grains compared to MI apatite allowed for stoichiometric chemical compositions to be measured successfully in two grains, showing that these apatite grains are enriched in F compared to Cl, with low OH contents (Fig 1).

Hydrogen isotope (D/H) ratios. MIL 090136 MI amphibole and apatite, as well as mesostasis apatite, were analysed for D/H ratios and H_2O abundances. The data show a clear distinction between the D/H ratios of

MI2 and mesostasis apatite ($\delta D = 690\text{--}1070\text{‰}$ vs. $330\text{--}470\text{‰}$, respectively) (Fig. 2). Water contents are variable within both apatite types, but the MI 2 apatite dataset extends to higher water contents than the mesostasis apatite ($H_2O = 4690\text{--}11240\text{ ppm}$ vs. $1120\text{--}5070\text{ ppm}$, respectively).

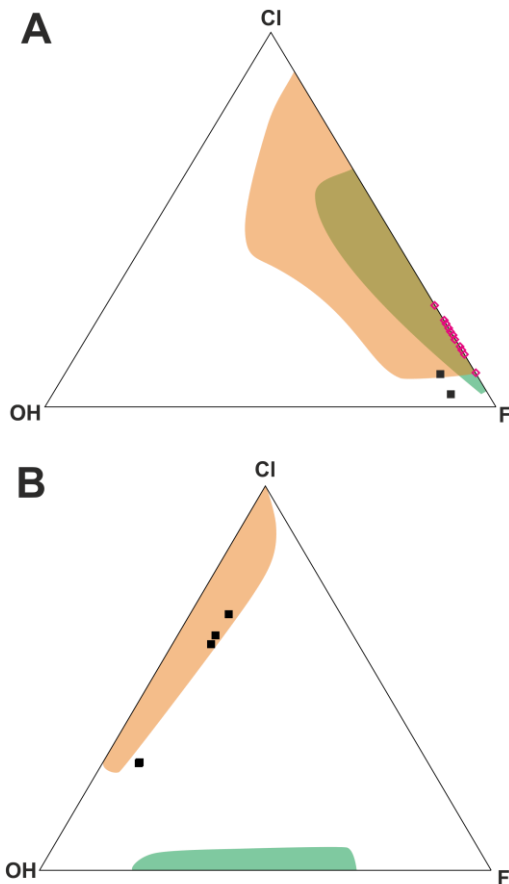


Fig. 1: Ternary plots showing apatite (A) and amphibole (B) compositions for MIL 090136 (black symbols). Orange and green envelopes represent previously reported nakhilite and chassignite data, respectively (see [2]). Pink symbols (A) show previously reported apatite data (all within the matrix) for the MIL nakhilites.

Two amphibole grains contain D/H and water contents similar to the MI2 apatite grains ($\delta D = \sim 900\text{‰}$ and $H_2O = \sim 3300\text{ ppm}$). These values are also in line with those reported for Chassigny MI amphibole and mesostasis apatite (Fig. 2; [9–10]). Similarly, the MIL 090136 mesostasis apatite water content is within the range shown for Nakhla apatite [11], although its D/H ratios are slightly higher.

Discussion: *The source of Cl-rich fluid in the nakhilites.* MIL 090136 MI amphibole and apatite have

intermediate D/H ratios, indicating that hydrogen, and the associated Cl, may have been sourced from the

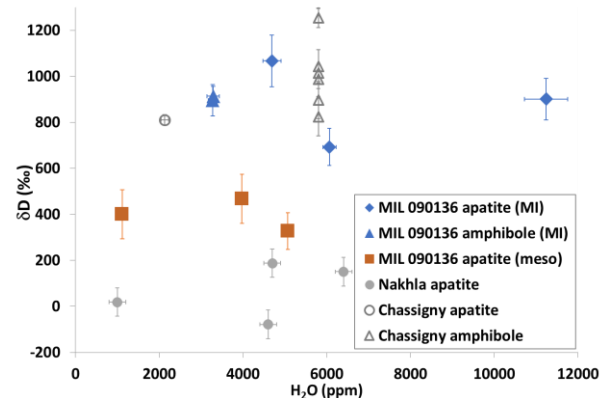


Fig. 2: D/H ratio (δD) vs. water content for MIL 090136 apatite and amphibole.

martian cryosphere, by assimilation of a perchlorate-rich fluid/ice/saltcrust during emplacement of the chassignite and nakhilite parental melt(s) in the martian crust (e.g., [12]). Perchlorate (ClO_4^-) at the surface of Mars was observed at the landing sites of the Phoenix lander and the MSL Curiosity rover [13–15]. Assimilation of perchlorate, or circulation of Cl-rich brines, is in agreement with the high bulk-rock $^{37}Cl/^{35}Cl$ ratios reported in the nakhilites (NWA 817 and 5790) and Chassigny [5,16–17] - recent analyses of $^{37}Cl/^{35}Cl$ ratios in early vs. late crystallizing apatite in Chassigny confirm that crustal assimilation was responsible for this change in Cl isotopic composition [5]. However, it is important to note that the water content of this perchlorate-rich source must have been minimal, as the bulk water content of the nakhilites is low [2, 18]. An assimilant with a high proportion of perchlorate saltcrust, as reported in [14], would fit this description.

References: [1] McCubbin et al. (2009) *GCA* 73, 4907–4917. [2] McCubbin et al. (2013) *MAPS* 48, 819–853 [3] Hallis (2013) *MAPS* 48, 165–179. [4] McCubbin and Nekvasil (2008) *Am. Min.* 93, 676–684. [5] Shearer et al., (2018) *GCA* 234, 24–36. [6] Barnes et al. (2013) *Chem. Geol.* 337–338, 48–55. [7] McCubbin et al. (2012) *Geology* 40, 683–686. [8] Barnes et al. (2014) *EPSL* 390, 244–252. [9] Watson et al. (1994) *Science* 265, 85–90. [10] Bocktor et al. (2003) *GCA* 67, 3971–3989. [11] Hallis et al. (2012) *EPSL* 359–360, 84–92. [12] Bellucci et al. (2017) *EPSL* 458: 192–202. [13] Hecht et al. (2009) *Science* 325, 64–67. [14] Cull et al. (2010) *GRL* 37, L22203. [15] Galvin et al. (2013) *JGR* 118, 1–19. [16] Sharp et al. (2016) *MAPS* 51, 2111–2126. [17] Williams et al. (2016) 51, 2092–2110. [18] Filiberto et al. (2014) 401, 110–115.